Modeling of a cloud tank

Matthias Schütze and Frank Stratmann

Leibniz Gemeinschaft

Leibniz-Institut für Troposphärenforschung, Permoserstr. 15, 04318 Leipzig, Germany

LEIBNIZ-INSTITUT FÜR TROPOSPHÄRENFORSCHUNG

Introduction

The investigation of real atmospheric clouds is rather difficult because of their high temporal and special variability. Laboratory studies under controlled and reproducible conditions are convenient means to understand the complex processes occurring during the lifetime of a cloud. These studies can be performed in large volume chambers which minimize wall effects. But it is a challenging experimental task to maintain homogeneous fields of thermodynamic and particle properties across the chamber volume.
This paper presents a newly developed modeling tool for the simulation of particle dynamics inside aerosol chambers. It is applied to a typical example of a cloud tank. Special emphasis is placed on the temporal and spatial inhomogeneities across the tank volume.

Model description

The Computational Fluid Dynamics (CFD) code FLUENT 6 was used to solve the coupled differential equations for vapor mass-transport, energy, and momentum. The Fine Particle Model (FPM) (Wilck et al., 2002; Particle Dynamics, 2003), an add-on module to FLUENT 6, was applied to account for particle dynamics. This combined CFD particle-dynamics model allowed the determination of vapor mass-fraction, temperature, flow velocity, particle number-concentration, and particle mass-concentration fields inside the cloud tank. The following processes are accounted for: vapor depletion due to condensation on particles and chamber walls, heat production on account of latent heat release associated with vapor condensation on particles, multi-component and thermal vapor diffusion, and particle transport by diffusion, thermophoresis, and sedimentation.
The realizable k-ε model with enhanced wall treatment provided by FLUENT was employed for the parameterization of turbulence.

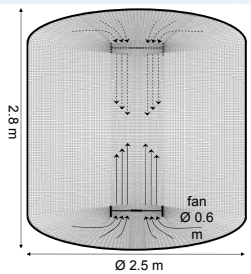

Fig. 1: Schematic of cloud tank. Gray lines show the grid.

Tank geometry

A standard geometry was chosen for the cloud tank, see Figure 1. It consists of a cylinder and two half oblate-spheroids on top and bottom. This geometry corresponds to a total volume of 12.4 m^3 and a surface area of 27.4 m^2. A fan, Ø 0.6 m, is placed at the center axis 0.45 m from the bottom of the tank. Optionally, a second fan is placed 0.45 m below the ceiling.

Mixing by fans

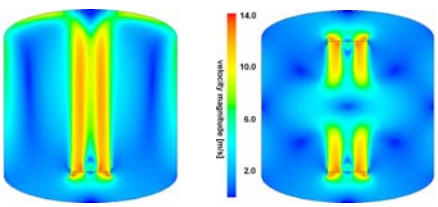

Fig. 2: Contour plots of the velocity magnitude for a one-fan (1x fan 2, left) and a two-fan configuration (2 x fan 2, right).

Different configurations of fans were investigated with respect to their capability to homogenize the tank volume. One or two fans with maximum velocities of either 7 m s^{-1} (= fan 1) or 13 m s^{-1} (= fan 2, see Fig. 2) were used.

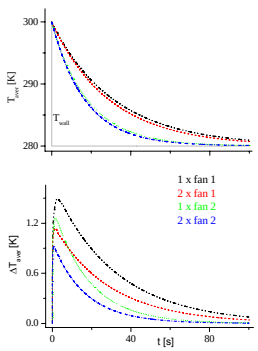

Fig. 3: T_{aver} and ΔT_{aver} after an instantaneous change of the wall temperature (gray line) for different configurations of mixing fans.

Fig. 3 shows the volume-averaged temperature T_{aver} and its volume-averaged standard deviation ΔT_{aver} after a step change of the wall temperature. Fig. 4 illustrates the inhomogeneities of the temperature that might be present in the tank.

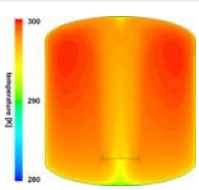

Fig. 4: T at t = 2.57 s for a '1xfan1' configuration. T_{aver}= 298.3 K, ΔT_{aver}= 1.5 K (cp. Fig. 3).

$(NH_4)_2SO_4$ particles in humid air

At t = 0 dry $(NH_4)_2SO_4$ particles (N = 10^9 m^{-3}, d_g = 50 nm, mono-disperse) were added to the tank volume (T = 299 K, pressure p = $1.01 \cdot 10^5$ Pa, mass fraction of water vapor x_{H_2O} = 0.02, corresponding water-vapor saturation S_w = 0.965) and allowed to equilibrate for 0.01 s.
Subsequently the air was pumped off from the tank for 100 s at a constant rate. This caused the thermodynamic parameters to change (adiabatic expansion), see top of Fig. 5. The figure also shows the response of the particle diameter (d_g) and number-concentration (N) to these changes. When the system starts to supersaturate with respect to water vapor, the particles start to grow dynamically.
After S_w drops below unity, the particles shrink and reach an equilibrium diameter again.
Figures 6 and 7 show the spatial distribution of the particle parameters across the tank at the times when their relative deviation is largest.

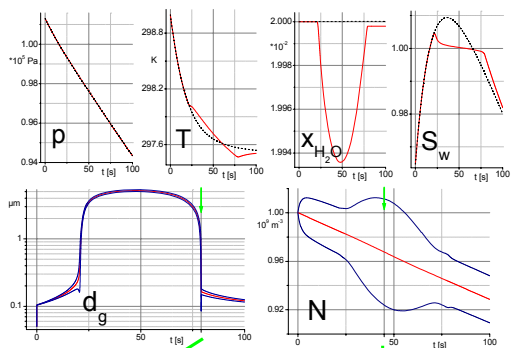

Fig. 5: Volume averages of p, T, x_{H_2O}, S_w, d_g, and N. red solid: with particles, black dashed: without particles, blue solid: value ± doubled stand. dev.

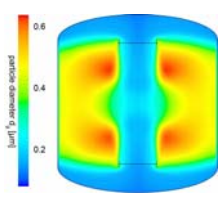

Fig. 6: Contour plot of d_g at t = 79.1 s when $\Delta d_{g,aver}/d_{g,aver}$ maximizes ($d_{g,aver}$ = 0.35 µm, $\Delta d_{g,aver}$ = 0.13 µm).

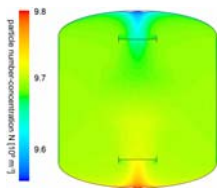

Fig. 7: Contour plot of N at t = 45.0 s when $\Delta N_{aver}/N_{aver}$ maximizes (N_{aver} = $9.67 \cdot 10^8$ m^{-3}, ΔN_{aver} = $2.20 \cdot 10^7$ m^{-3}).

Literature

Particle Dynamics (**2003**) FPM Users Guide, http://www.particle-dynamics.de, Particle Dynamics GmbH, Leipzig, Germany
Wilck, M., Stratmann, F. and Whitby (**2002**) A fine particle model for FLUENT: Description and application,), Proc. 6th Int. Aerosol Conf., Taipei, Taiwan, Chinese Association for Aerosol Research in Taiwan/ International Aerosol Research Assembly, 1269.